

Molecular Orientational Order of Nitroxide Radicals in Liquid Crystalline Media

N. A. Chumakova,[†] T. S. Yankova,[†] K. E. Fairfull-Smith,[‡] S. E. Bottle,[‡] and A. Kh. Vorobiev^{*,†}

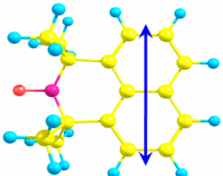
[†]Department of Chemistry, M. V. Lomonosov Moscow State University, Moscow 119991, Russian Federation

[‡]School of Chemistry, Physics and Mechanical Engineering, Faculty of Science and Engineering, Queensland University of Technology, GPO Box 2434, Brisbane, QLD 4001, Australia

Supporting Information

ABSTRACT: The orientational distribution of a set of stable nitroxide radicals in aligned liquid crystals 5CB (nematic) and 8CB (smectic A) was studied in detail by numerical simulation of EPR spectra. The order parameters up to the 10th rank were measured. The directions of the principal orientation axes of the radicals were determined. It was shown that the ordering of the probe molecules is controlled by their interaction with the matrix molecules more than the inherent geometry of the probes themselves. The rigid fused phenanthrene-based (A5) and 2-azaphenalene (A4) nitroxides as well as the rigid core elongated C11 and 5 α -cholestane (CLS) nitroxides were found to be most sensitive to the orientation of the liquid crystal matrices.

Order parameters	Orientation axis
$\langle P_{20} \rangle$	0.738
$\langle P_{40} \rangle$	0.517
$\langle P_{60} \rangle$	0.281
$\langle P_{80} \rangle$	0.139



I. INTRODUCTION

Admixtures to liquid crystalline (LC) media are widely used for the development of new materials such as polymer-dispersed liquid crystals (PDLS)^{1–3} or polymer-stabilized mesophases.^{4,5} In addition, admixture molecules can be introduced into liquid crystals to investigate the properties of the medium. The research use of admixture molecules is based on the molecular probe technique, where properties of specially introduced guest molecules are measured to characterize the medium. In particular, light-absorbing and light-emitting probe molecules (dyes) are used, mainly for determination of the second rank order parameters and rarely for estimation of fourth rank order parameters of liquid crystals by means of optical measurements.^{6–14} More detailed information concerning the molecular orientational order in liquid crystals and characteristics of molecular motions in the studied media, however, can be extracted by using stable paramagnetic molecular additives (spin probes) in combination with EPR spectroscopy.^{15–19} To date, there is only a limited set of substances that have been applied as optical and paramagnetic probes. These probes have been chosen by empirical, trial-and-error experiments with the implicit assumption that the main cause of orientational alignment in the ordered medium arises from the elongated shape of the molecules. Consequently, a number of elongated probe molecules have traditionally been employed for the investigation of the liquid crystals. On the other hand, it is known that compact piperidine spin probes (TEMPONE, TEMPOL, etc.) also demonstrate considerable orientational ordering in LC media in spite of an almost circular, non-elongated molecular shape.^{20–22} Therefore, the shape of the dopant molecules is not the only factor that governs molecular orientation of the probes doped into liquid crystals. Thus, it is necessary to ascertain real orientation axis of the guest

molecule, i.e., the molecular axis that is ordered in the aligned liquid crystal to the maximum extent.

Another assumption that is commonly made when using probe additives in LC media is the concept of equivalence for all of the guest molecules. Indeed, all probe molecules are ideally considered to be completely identical particles, all exposed to the same surroundings. In actual fact, LC media are orientationally ordered in the case of nematic mesophases or orientationally and spatially ordered in the case of smectic mesophases. It is logical to expect that the same probe molecules occupy different host–guest orientations in the differing locations within LC medium.

Thus, the aim of this work is to investigate the factors that control the orientation of guest molecules in anisotropic LC media. Deeper understanding of such factors would be of value for the selection of the most effective probe substances and for the development of LC composition materials with desired properties. For this purpose, standard nitroxide spin probes as well as novel stable nitroxide radicals with different molecular shapes were applied. The nematic 4-*n*-pentyl-4'-cyanobiphenyl (5CB) and smectic 4-*n*-octyl-4'-cyanobiphenyl (8CB) were used as model liquid crystalline media.

The orientation distributions of the radicals in the aligned samples were determined in detail by means of EPR spectroscopy. Before the spectra were recorded, the aligned samples were snap-frozen to prevent the reorientation of nematic phases along the magnetic field of EPR spectrometer during the angular dependence acquisition. The second advantage of frozen samples is the more simple simulation of rigid limit spectra EPR in comparison with simulation of spectra for rotating radicals.

Received: November 29, 2013

Revised: April 30, 2014

Published: April 30, 2014



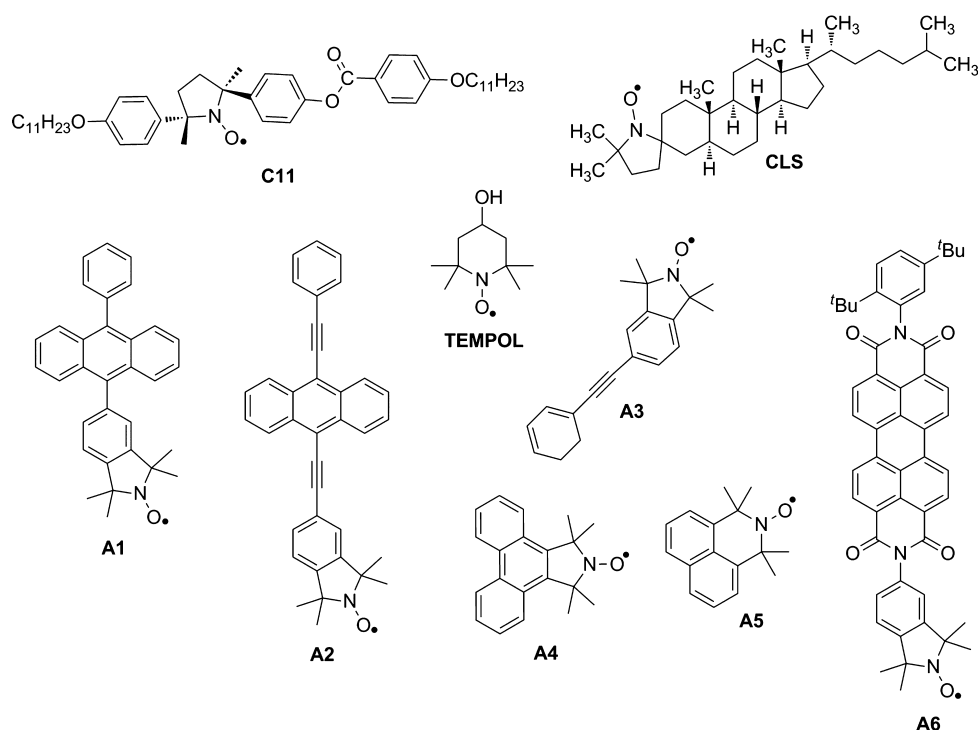


Figure 1. Nitroxide radicals used in the present work.

Liquid crystals often form a supercooled glassy state with conservation of molecular order under rapid cooling.^{23–27} This technique was shown previously to produce reliable and detailed orientational molecular characteristics such as order parameters and the angles which define the orientation axes of molecules.^{13,18,28}

II. EXPERIMENTAL AND COMPUTATIONAL METHODS

Materials and Reagents. Liquid crystals 5CB and 8CB were obtained from Merck and used without further purification. The phase transition temperatures for these materials were measured using a polarizing optical microscope MIN-8 equipped with a temperature control unit. The temperature range for the formation of the nematic phase was 293–320 K which is in accordance with literature reports.^{29,30} 8CB showed nematic and smectic phases within the ranges of 306–314 K and 294–306 K correspondingly, which are close to the known properties of these materials.^{29,31}

The structures of the nitroxide radicals examined in this study are presented in Figure 1. The radicals 2,2,6,6-tetramethyl-4-ol-piperidinoxyl (TEMPOL) and 3 β -DOXYL-5 α -cholestane (CLS) were obtained from Aldrich and used without further purification. The synthetic procedures used to prepare radicals C11,^{32,33} A1 and A2,³⁴ A3,³⁵ A4,³⁶ and A5³⁷ have been described previously. Radical A6 was prepared from 3,4,9,10-perylene-tetracarboxylic dianhydride in a manner similar to that previously reported.³⁸

Preparation of the Samples. Quartz ampules for EPR measurements (3 mm diameter) were filled with liquid crystals containing the spin probes, evacuated at pressure 10^{-3} Torr, and sealed. The spin probe concentration was $\sim 1 \times 10^{-3}$ mol/L. Two types of samples were studied. The unordered samples were prepared by heating above the clearing temperature followed by rapid cooling down to 77 K. Samples with orientational order were prepared by heating the material to the temperature of the

mesophase, exposing for 5 min to a 0.5 T magnetic field of an EPR spectrometer at that temperature, and then rapidly cooling to 77 K while keeping within the magnetic field. The freezing was realized by immersion of the ampule in liquid nitrogen. Aligned samples with the symmetry axis directed perpendicular to the ampule axis were obtained in this way. It was confirmed by separate experiments that the orientational order of both 5CB and 8CB reached saturation using a field of 0.3 T. It was also confirmed that the order of the liquid crystals remained constant when held at 77 K for periods of at least several days.

EPR Measurements. X-band EPR spectra were recorded with a Varian E3 EPR spectrometer over temperatures ranging from 105 to 380 K. A Varian E-4557-9 temperature control unit (with an accuracy of ± 1 °C) was used. The W-band EPR measurements were performed using a Bruker E680 spectrometer. The temperature of the sample was maintained at 100 K using an Oxford Instrument (model CF935) helium flow cryostat with an Oxford Instrument (model ITC500) cryostat controller. Spectra of the macroscopically ordered samples were recorded at different angles between the sample anisotropy axis and the direction of the magnetic field using 10° increments. The turn angle was set up using a goniometer with an accuracy of $\pm 2^\circ$.

All spectra were normalized to the area under the absorbance curves, and the normalized spectra were used for numerical fitting. The accuracy level of experimental recording of the EPR spectra was estimated using the spectral ranges where the signals are negligibly small (“tails” of spectra). The mean squared deviation arising from the experimental noise in the range of the “tails” was used as a level of recording accuracy (F_{err}). This value was used in course of spectra fitting for determination of validity of parameters. Any new adjustable parameter was considered to be significant only if the minimum χ -squared was improved by more than the value of F_{err} .

Quantum Chemical Computation. The computation of the molecular geometry of the radicals under consideration was

Table 1. Magnetic Resonance Parameters of the Studied Radicals

radical	$g_{\text{iso}} \pm 0.0002$	$A_{\text{iso}} \pm 0.05 \text{ G}$	$g_{\text{xx}} \pm 0.0002$	$g_{\text{yy}} \pm 0.0002$	$g_{\text{zz}} \pm 0.0002$	$A_{\text{xx}} \pm 0.3$	$A_{\text{yy}} \pm 0.3$	$A_{\text{zz}} \pm 0.05$
A1	2.0062	14.69	2.0092	2.0068	2.0025	5.3	4.3	33.15
A2	2.0059	14.78	2.0090	2.0062	2.0024	4.2	4.7	33.70
A3	2.0062	14.61	2.0093	2.0065	2.0028	4.5	6.5	32.98
A4	2.0061	14.76	2.0091	2.0066	2.0026	3.2	6.5	33.34
A5	2.0063	15.71	2.0097	2.0068	2.0023	7.0	4.8	34.17
A6	2.0058	14.54	2.0083	2.0067	2.0025	<5.6	5.5	33.43
C11	2.0058	13.50	2.0091	2.0060	2.0022	4.0	5.3	32.10
CLS ^{46,a}	2.0055	14.50	2.0087	2.0057	2.0021	4.9	5.5	33.10
TEMPOL	2.0061	15.82	2.0099	2.0062	2.0022	6.7	6.4	34.32
TEMPOL ⁴⁵	2.0062	15.60	2.0099	2.0063	2.0022	6.2	7.0	34.30

^aMagnetic parameters for cholestane probe were taken from ref 46.

performed using the ORCA software package.³⁹ The computational model B3LYP/N07D was used for optimization.⁴⁰ The medium of toluene at 293 K was taken into account within continuum approximation.⁴¹ The model was specially tested on three stable nitroxide radicals: 2,2,6,6-tetramethylpiperidin-1-oxyl, 4-hydroxy-2,2,6,6-tetramethylpiperidin-1-oxyl, and 3-carbamoyl-2,2,5,5-tetramethyl-3-pyrrolin-1-oxyl. The values of bond lengths and valence angles, optimized according to B3LYP/N07D, were compared with the experimental structural data determined by X-ray diffraction.⁴² It was found that deviations of the calculated data from experimental values were no more than 10^{-3} nm and 0.5° , respectively.

The calculated optimal geometry for the radicals studied in the present work is presented in the Supporting Information (Table S2). Two probe molecules used (C11, CLS) carry the flexible side substitutes. The conformations of these substitutes were not considered in detail assuming that their equilibrium geometry is achieved by ordering action of LC medium and does not influence significantly on the orientation of rigid part of molecule. The possible intramolecular rotations of larger fragments of probe molecules (for instance, terminal benzene rings in the C11, A1, and A6) were studied by calculation of dependencies of energy on rotation angle. Results of these calculations are presented in the Supporting Information (Figures S1, S2 and S3). The results demonstrate that intramolecular rotations in A1 and A6 are hindered and characterized by rather large activation energy (50–80 kJ/mol). The intramolecular rotations in A2, A3, and C11 were shown to occur with low activation energy (~ 4 –8 kJ/mol). Thus, up to a 20% admixture of twisted molecular conformations can be expected. However, the elongated shape of these molecule and inertia moments are insignificantly changed in the course of the possible intramolecular rotations (Table S1, Supporting Information). Thus, the probes used can be considered as essentially rigid and each probe is described by sole molecular geometry.

EPR Spectra Simulation. The in-house generated software package as described in ref 18 (available from ref 43) was used for the quantitative simulation of EPR spectra. The determination of spectral parameters was performed by nonlinear-least-squares fitting with minimization of the discrepancy between calculated and experimental spectra. Newton-type adaptive algorithm NL2SNO⁴⁴ was used for minimization procedure. Calculation of EPR spectra was performed in a weak external field approximation up to the second order of the perturbation theory. Individual line shape was described by convolution of Gaussian and Lorentzian functions. Gaussian and Lorentzian line widths were second rank tensors, which were used to take

into account the anisotropy of line widths. The principal axes of hyperfine interaction tensor as well as the line width axes were assumed to coincide with the g -tensor principal axes. Since the experimental spectra were recorded at the temperature 105 K, the calculation of spectra was performed with the assumption of the absence of radical rotational movement (in rigid limit). The method used for the simulation of EPR spectra at the rigid limit is discussed in detail in previous work.¹⁸

In the present work, two types of EPR spectra simulations were performed. The values of magnetic parameters as well as the shape and the width of individual resonance lines were obtained by means of the simulation of the EPR spectra of unordered samples. The simulation of the EPR spectra angular dependences of the aligned samples was used for the determination of the orientation distribution functions of the radicals in liquid crystals.

Determination of Magnetic Parameters. Values of isotropic g -factor and constants of hyperfine structure (HFS) were determined from the EPR spectra of radical solutions in 5CB at 380 K. The standard samples of 2,2-diphenyl-1-picrylhydrazyl (DPPH) and Mn^{2+} in a crystal lattice of magnesium oxide were used for these measurements. The data obtained are given in Table 1.

A numerical simulation of the spectra recorded at 105 K was used for the determination of the anisotropic magnetic parameters. It was found that the obtained values for the components of g - and HFS-tensors in the case of radicals A5, C11, and TEMPOL are close to the typical values for nitroxide radicals.⁴⁵ For the widely used spin probe TEMPOL, the obtained values were in agreement with the literature data for a solution of TEMPOL in toluene (see Table 1). However, simulation of the spectra in the case of radicals A1, A2, A3, A4 and A6 resulted in several minima of approximately the same depth with different optimal magnetic parameters. In one of these alternative parameter sets, the anisotropy of the g -tensor was often close to axial ($g_x \sim g_y$) which is not typical for nitroxides and calls into question the reliability of the simulation for these molecules. For a more accurate determination of the g -tensors, W-band EPR spectra for radicals C11, A2, A3, A4, and TEMPOL were recorded and simulated. These experiments and simulation have shown that all radicals under consideration have g -tensors that are common for nitroxides. As an example, in Figure 2 the X-band and W-band spectra of radicals C11 and A2 in 5CB as well as the results of their computer simulation are shown. The parameters obtained are presented in Table 1.

Determination of Orientation Distribution Functions of the Radicals in Aligned Liquid Crystals. Orientation distribution functions were determined by the joint numerical

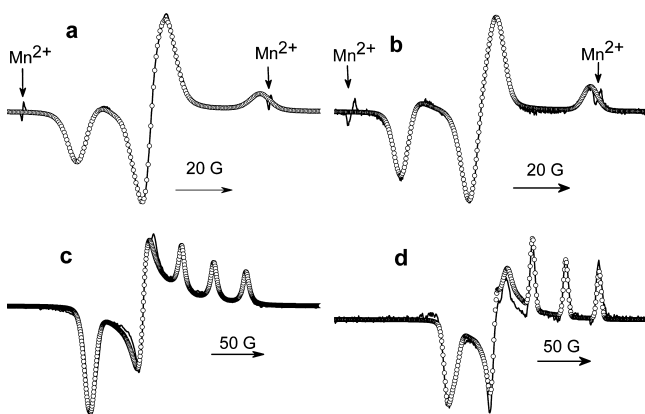


Figure 2. X-band (a, b) and W-band (c, d) EPR spectra of unordered samples of radicals C11 (a, c) and A2 (b, d) in liquid crystal SCB and results of their numerical simulation (lines are experimental spectra, circles are simulated spectra).

simulation of set of 10–20 EPR spectra recorded at different angles between the director of the sample and the magnetic field vector. The method is described in detail in previous work.¹⁸

Two different orientation distribution functions were determined in the present work for each sample. First is the distribution of the molecular *g*-tensor axes in uniaxial LC medium. This distribution can be expressed by the following series^{6,47}

$$\rho(\beta, \gamma) = \sum_{j=0}^{\infty} \left[\frac{1}{2} a_{j0} P_j(\cos \beta) + \sum_{k=1}^j a_{jk} P_j^k(\cos \beta) \cos(k\gamma) \right] \quad (1)$$

where $P_j(\cos \beta)$ are Legendre polynomials, $P_j^k(\cos \beta)$ are associated Legendre functions, and angles β and γ characterize orientation of the sample symmetry axis in the magnetic reference frame of the molecule.

In the case of the distribution function described by eq 1, coefficients a_{jk} were the parameters varied in the course of fitting of the EPR spectra. These coefficients are order parameters for magnetic axes of probe molecule. For description of the distribution by eq 1 up to rank 10, the common number of parameters reaches 20. The coefficients with higher indices j and k , as a rule, were very close to zero. Thus, the real number of the parameters varied to describe simultaneously 12–15 spectra was no more than 15.

The distribution (1), however, is not very informative when the characteristics of orientation axes of probe molecule are examined. The distributions of molecular orientation axes are the second type of characteristics obtained in the present work. The determination of such distributions is based only on the assumption that there exists the molecular frame with the axes being the principal directions for ordering matrix of any rank. Axes of this orientational frame must, obviously, coincide with the principal axes of Saupe second rank ordering matrix. The axes of the molecular orientational frame are determined not only by symmetry of probe molecule but by symmetry of anisotropic medium and nature of specific interactions of the probe molecule with the medium. In general, the orientational molecular frame is related with *g*-tensor frame of probe molecule by three Euler angles ϕ , θ , and ψ . It was found earlier¹⁸ and confirmed in the present work that orientational molecular frame is uniaxial in majority of studied cases. In these

cases EPR spectra are independent of angle ψ and only angles ϕ , θ describing the direction of main molecular orientation axis are important. The orientation distribution for such cases is expressed as follows^{6,47}

$$\rho(\delta) = \sum_{l=0}^{\infty} \frac{2j+1}{2} \langle P_j \rangle P_j(\cos \delta) \quad (2)$$

where δ is the angle between the molecular orientation axis and the liquid crystal director, $P_j(\cos \delta)$ are Legendre polynomials, and $\langle P_j \rangle$ is order parameter of rank j (angle brackets indicate averaging over all molecular orientations).

Order parameters $\langle P_j \rangle$, as well as angles θ and φ , were determined by fitting of experimental angular dependence of EPR spectra. The seven parameters of distribution function (2) up to rank 10 were varied in course of the fitting. It should be stressed that eq 2 is valid when the probe molecule demonstrates only one orientational molecular axis, in other words, when the molecule is characterized by a uniaxial orientational tensor. The uniaxiality of the orientational tensor means that the probability of finding a molecule with that orientation, which can be obtained by rotation around main orientation axis, is the same. In such cases, the results of the spectral simulation obtained from applying expressions (1) and (2) proved to be the same. When this equivalence is violated, the distribution (2) becomes inapplicable. The expression relating functions (1) and (2) was obtained elsewhere:¹⁸

$$a_{jm} = \langle P_j \rangle \frac{(-1)^m (j-m)!}{(j+m)!} \cos m\varphi P_{jm}(\cos \theta) \quad (3)$$

Examples of spectral simulations and the distribution functions obtained are presented in Figure 3.

The orientation distribution of radical A3 in aligned liquid crystal SCB is shown in Figure 3b in the form of eq 1. The function is presented as a 3D figure which maps the distribution of the sample symmetry axis in relation to the molecular reference frame (principal axes *g*-tensor frame). The symmetry of the distribution reflects the limitations of the method. It is known that nitroxide radicals possess orthorhombic magnetic symmetry. This means that for every direction in the molecular frame, there are seven other directions, none of which can be distinguished by means of EPR spectroscopy. These directions can be transformed one to other by symmetry operations. The “lobes” which one can see in Figure 3b correspond to the indistinguishable directions caused by orthorhombic symmetry. Reflections of every lobe in mirror planes *XY*, *XZ*, and *YZ* produce the observed shape of the distribution. When expression (2) is used to calculate the orientation distribution function, the distribution is seen as two lobe with the axis directed with certain angles (θ , φ) (Figure 3c). The indistinguishable directions in this case correspond to the angles sets $(\pm\theta, \pm\varphi)$.

It is necessary to focus specifically on the determination of the rank of expansions (1) and (2). Truncated series (1) and (2) were used for these simulations. To choose the number of terms required we performed fitting of each set of spectra several times applying a sequential increase in the expansion rank. Each time we compared the value of the decrease of deviation of calculated spectra from the experimental data caused by addition of next rank terms and the value of the error of the spectra registration F_{err} . When the decrease of deviation does not exceed the value of experimental error, it means that truncation of series is optimized and the next terms are not required for an accurate simulation. The significance for each

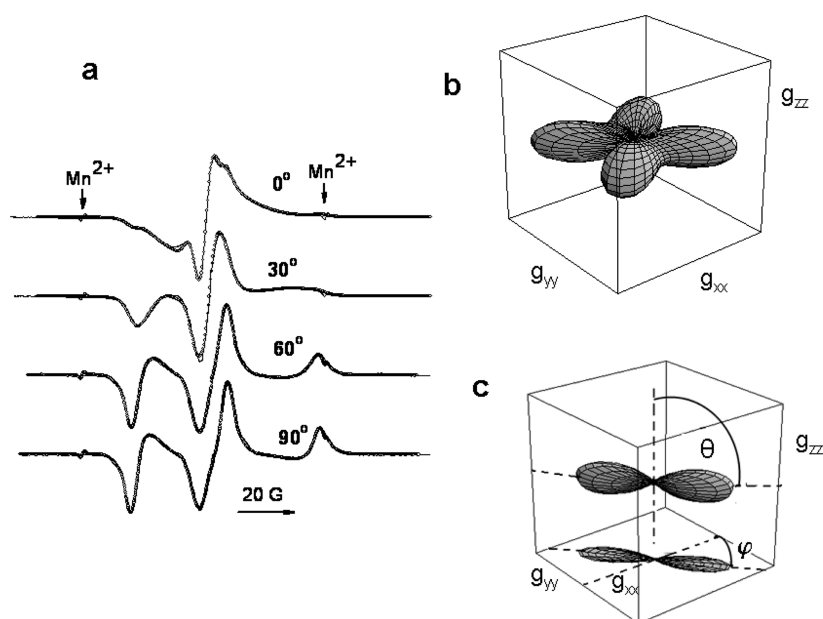


Figure 3. (a) Experimental EPR spectra of radical A3 in aligned liquid crystal 5CB, recorded at 105 K at different angles between the director of the sample and the magnetic field vector (lines) and results of simulation (circles); orientation distribution functions (b) in the form of eq 1 and (c) in the form of eq 2.

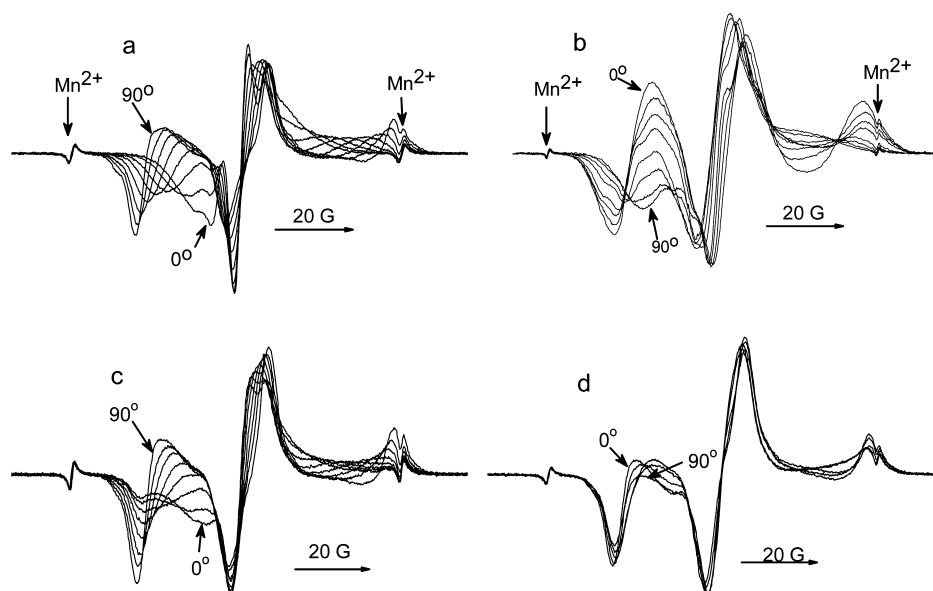


Figure 4. EPR spectra of the radicals A4 (a), C11 (b), A2(c), and A1(d) in aligned liquid crystal 5CB, recorded at different angles between the magnetic field vector and the liquid crystal director.

individual higher coefficients in eq 1 was determined using the same way.

III. RESULTS AND DISCUSSION

The orientation distribution functions were determined in the present work by means of joint numerical simulation of the EPR spectra recorded at different angles between the magnetic field vector and the liquid crystal director. The examples of experimental EPR spectra recorded for some of studied samples are shown in Figure 4. It can be seen that different radicals demonstrate considerably different angular dependence in the EPR spectrum.

For qualitative understanding of the orientational characteristics reflected in spectra in Figure 4 it should be taken into

account the following. The nitroxide radicals oriented along the magnetic field by their magnetic z -axis produce the three-line subspectrum with a large distance between the components, while lines of subspectra from radicals oriented along the magnetic field by x and y axes lie significantly closer. As the observed EPR spectrum is the superposition of subspectra originating from all radicals, the large outermost components indicate the large number of radicals with z orientation. For example, such a spectrum is seen in Figure 4a for 90° direction of the sample relative to magnetic field. It means that radical A4 mainly oriented by its z axes perpendicular to director of LC. Other spectra of angular dependence can be analyzed in the same way. However, the quantitative data concerning orientation

distribution can be obtained only by numerical simulation of the spectra. The function in the form (1) is the orientation distribution of sample director in the magnetic reference frame of the molecule. The orientation distribution functions for radicals A1, A2, A3, A4, A6, and C11 in aligned 5CB are presented in Figure 5.

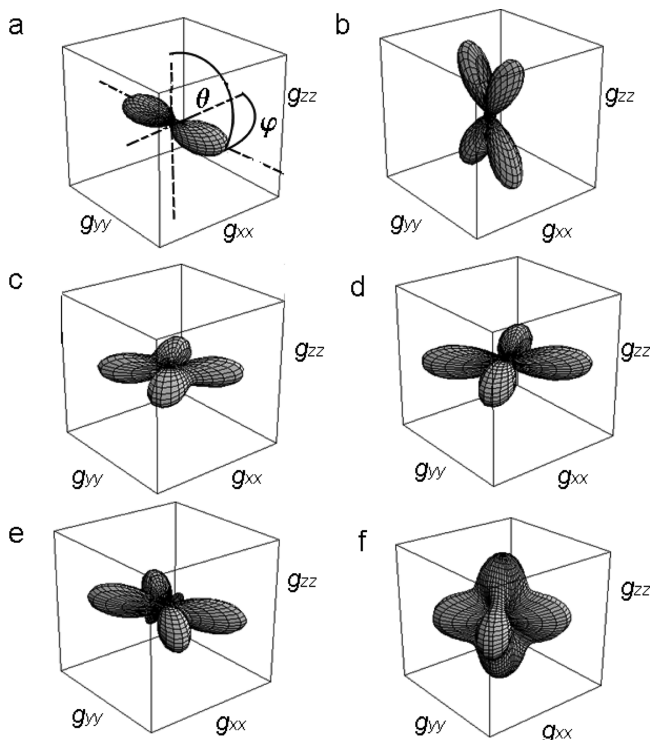


Figure 5. Orientation distribution functions of radicals A4 (a) C11 (b), A3 (c), A6 (d), A2 (e), and A1 (f) in aligned liquid crystal 5CB. The distributions are presented in reference frames of the radicals.

In Figure 5a, the paramagnetic molecules A4 are ordered along the director of the LC medium by their magnetic Y axes. In this case, indistinguishable directions are superimposed onto each other and form together a two-lobe distribution. The very similar EPR spectra and distribution function was obtained for probe A5. In the cases of these radicals LC director lies in the plane of molecule mainly perpendicular to NO bond of nitroxide moiety.

The molecules C11 (Figure 5b) are oriented so that the liquid crystal director lies in the XZ plane of the molecular g-tensor. As a result, the orientational distribution extracted from the EPR spectra in this case consists of four lobes.

The orientation distribution of radicals A3 presented in Figure 5c shows that radicals are oriented mainly in such a way that the director lies in XY plane of g-tensor. This four-lobe distribution in the XY plane is similar to the four-lobe distribution of radical C11 in the XZ plane. Radicals A6, A2, and A1 resemble radical A3. All these substances include the same isoindoline moiety, which carries the nitroxide group. Positions of these isoindoline groups relative to the longest molecular axes are approximately the same. Therefore, it is reasonable to suppose that orientation functions of these radicals would be similar. Indeed, the function of A6 (Figure 5d) looks like the function of A3. The orientation distribution function of radicals A2 (Figure 5e) is in general similar to the functions of A3 and A6, but in the central part of this function one can

observe two small additional lobes corresponding to the molecules oriented along the LC director by their magnetic X axes. This additional two-lobe distribution is not connected with the four-lobe main part of the distribution. Thus, this additional distribution function indicates that a minor fraction of the guest molecules demonstrate a distinct kind of orientational order in the same media. The similar feature becomes very appreciable in the case of the distribution of radical A1 in 5CB shown in Figure 5f. It can be seen that the orientation distribution of A1 particles in the XY plane is a four-lobe orthorhombic function similar to functions considered above. However, a large part of the molecules are ordered along the LC director by their Z axes and form an additional two-lobe distribution function. Thus, there are two orientations of the paramagnetic molecules relative to the liquid crystal director. These observations clearly indicate that guest molecules can be oriented in LC media in two or more distinct manners.

The orientation distribution functions both in form (1) and in form (2) describe orientational order quantitatively. However, the coefficients a_{jk} of expression (1) describe ordering of the magnetic axes of the probe molecules whereas coefficients $\langle P_j \rangle$ of expression (2) describe order of the orientational molecular axis. Thus, the model (2) allows obtaining more informative characteristics of the ordering of guest molecules in the sample. This question is discussed in detail in ref 18. On the other hand, the model (2) cannot be used when there are several different modes of orientation because the orientation distribution in this case does not possess the axial symmetry. The probe A1 demonstrates such behavior. Formally radical A2 also has a double-mode distribution, but in this case the part of molecules consisting additional two-lobe distribution is so small that model (2) can be applied approximately for analysis of this system.

Quantitative Characteristics of Orientational Order.

As described above, the samples studied were prepared by rapid freezing of ordered liquid crystals by immersion of the ampule in liquid nitrogen. It was found that the EPR spectra of frozen samples are independent of temperature of mesophase before the freezing. This observation is conformed to published evidence that the lower temperature smectic A or smectic C mesophase is stabilized in supercooled state in frozen sample.²⁵ In our experiments, the supercooled state of 5CB was a nematic glassy state, but the structure of frozen 8CB corresponds to overcooled smectic A mesophase. It is known that structural relaxation in course of cooling of glassy-forming liquids ceases in the vicinity of glass-transition temperature T_g . The value of T_g for many supercooled liquid crystals was measured,^{25,27} but it was found to be dependent on rate of cooling.⁴⁸ We believe that supercooled glassy mesophases 5CB and 8CB in our experiments correspond to temperature close to temperature of crystal-mesophase transition. The values of order parameters for glassy mesophases, which are almost equal to order parameters for the low temperature limit of mesophase existence, were determined earlier for a number of liquid crystals.²⁶

The values of order parameters measured in the present work for orientation axes of radicals and the values of angles (θ , φ) describing the direction of these orientation axes in g-tensor frames are collected in Table 2. In the case of probe A1, both in 5CB and 8CB, double-mode distribution is realized. For this reason, the angles (θ , φ) for A1 were determined approximately on the basis of the distribution described by expression (1). The order parameters of orientation axis in this case cannot be determined. The order parameters for magnetic z-axis of A1 are

Table 2. Order Parameters and Direction Angles for Orientation Axes (Errors Are Given in Parentheses)^a

	A1 ^b 5CB	A1 ^b 8CB	A2 5CB	A2 8CB	A3 5CB	A3 8CB	A4 5CB	A4 8CB	A5 5CB	A5 8CB	A6 5CB	A6 8CB	CLS 5CB	C11 5CB	TEMPOL 5CB
$\langle P_2 \rangle$	0.039	-0.009	0.554	0.615	0.643	0.738	0.763	0.665	0.612 (0.012)	0.625 (0.034)	0.713	0.629	0.399	0.629	0.433
$\langle P_4 \rangle$	0.077	0.057	0.293	0.244	0.355	0.517	0.506	0.276	0.335 (0.021)	0.300 (0.057)	0.399	0.322 (0.04)	0.184	0.322 (0.04)	0.277
$\langle P_6 \rangle$			0.125	0.058	0.142	0.281	0.289	0.056	0.183 (0.031)	0.108 (0.052)	0.184	0.165	0.082	0.165	0.174
$\langle P_8 \rangle$			0.063	0.015	0.051	0.139	0.100	0.013	0.101 (0.041)		0.082	0.060	0.013	0.060	
$\langle P_{10} \rangle$						0.051									
θ (deg)	~86 (1st type of ordering)	~90 (1st type of ordering)	90.0	89.9	89.9	90.0	99.1	89.8 (5.8)	98.0	97.0 (4.1)	93.0	30.6	75.5		
	~0 (2nd type of ordering)	~0 (2nd type of ordering)													
φ (deg)	~54 (1st type of ordering)	~51 (1st type of ordering)	58.5	56.8	50.8	74.9	90.0	98.5	42.8	33.0	66.9	90.6(5.9)	65.1		

^aErrors in the determination of order parameters were typically ~ 0.01 . Errors for angles θ and φ were usually less than $1-2^\circ$. When error values exceeded these levels they are presented in parentheses.

^bThe values of order parameters for z-axis of A1 are presented.

presented in Table 2. The small values of these parameters reflect the existence of double-mode orientation, but these values cannot be compared with the order parameters presented in Table 2 for other radicals.

The values of order parameters given in Table 2 for all spin probes except A1 can be compared with the literature values for aligned 5CB and 8CB. Only order parameters of rank 2 (values $\langle P_2 \rangle$) and rarely parameters of rank 4 (values $\langle P_4 \rangle$) were measured as a result of limitations of optical techniques. It is known that order parameter $\langle P_2 \rangle$ for nematic 5CB and smectic 8CB can reach values of 0.57–0.65^{29,49–55} and 0.56–0.62,^{55,56} respectively. Therefore, the values $\langle P_2 \rangle$ which were obtained in the present work involving several different spin probes correlate well with existing literature data. One exception is the parameter $\langle P_2 \rangle$ which was obtained for the radical TEMPOL. The literature data concerning the values of parameter $\langle P_4 \rangle$ for 5CB and 8CB are not in agreement^{52–55} as they lie in the interval from 0.09⁵⁴ to 0.36.⁵³ It should be noted that all values $\langle P_4 \rangle$ obtained in present work are no less than 0.24.

Values of high-rank-order parameters (6th, 8th, 10th) presented in Table 2 provide a more detailed description of orientational order than the commonly used second- and fourth-rank-order parameters. The values of high-rank-order parameters reflect subtle features of orientation distribution, which cannot be characterized by values of $\langle P_2 \rangle$ and $\langle P_4 \rangle$. Indeed, values of high-rank order parameters are not proportional to the value of $\langle P_2 \rangle$. For example, in the case of radical A2, the value of $\langle P_2 \rangle$ for 8CB exceeds the value for 5CB. On the contrary, the values of $\langle P_4 \rangle$, $\langle P_6 \rangle$, and $\langle P_8 \rangle$ for 8CB are less than the corresponding values for 5CB.

The data presented in Table 2 provoke discussion concerning the nature of order parameters obtained. Unfortunately, the meaning of order parameter for host molecule of liquid crystals is not quite definite. Indeed, the ordering of different fragments of the liquid crystal molecules, for instance, aromatic rings and hydrocarbon substitutes can be, in general, significantly different. Thus, values of the order parameter measured using different physical molecular properties can differ. In the case of the smectic mesophase this difference is transformed into spatial inhomogeneity of order parameter value, as the molecular order in layers is likely to differ from the molecular order present in interlayer space. This indefiniteness becomes even more in the case of using of probe technique. The different probe molecules, depending on each individual chemical structure, are preferentially bound close to certain structural features of the host medium or they are arranged in local molecular structures. Such a dependence of results on the localization of probe molecules is a specific property of the spin probe technique. The sensitivity to the local properties of medium is simultaneously a drawback and an advantage for all probe methods. This feature complicates the extraction of characteristics averaged on the medium as a whole, but provides important information concerning the local structure and properties of medium. Taking into account the possible different localizations of probe molecules and their different anisotropic interactions with host molecules one can expect the variation of order parameter value for different probes. This expectation is, as a whole, in accordance with the data presented in Table 2. Indeed, the values of order parameters obtained with the use of different probes for the same medium differ in some degree. The obtained values for certain probes are smaller than order parameter of host molecules measured by other methods but for other probes they are somewhat greater. On the other hand,

the order parameters presented lie in the narrow range mainly. The values of $\langle P_2 \rangle$ were found to be close to the literature data. Thus, the majority of tested spin probes reflect the LC ordering well.

At any rate, one can expect that the more is similarity between the structures and properties of host and probe molecules, the closer should be their orientational order. In accordance with the obtained results, radicals A4, A5, and CLS demonstrate the greatest values of order parameters. This is probably because the radicals A4 and A5, on the one hand, have fused aromatic systems which lead to some kind of stacking interactions with the molecules of cyanobiphenyl. On the other hand, the shape of these radicals is compact and they can easily be embedded in the structure of liquid crystal. Radical CLS which has elongated shape and considerable length may be seen as “averaging” probe. Since the molecular length of CLS molecule is substantially longer than 5CB or 8CB molecules, this probe must reflect an averaged orientation of several neighboring LC molecules.

Radicals A2, A3, A6, and C11 show the close values of order parameters. The difference between these values is comparable with the errors of the determination. Similarity of order parameters of probes A2, A3, and A6 is more likely connected with their similarity in structure. It is necessary to note that in the case of radical A2 the values of order parameters are somewhat underestimated as the result of admixture of small additional orientation of the radicals along the LC director by their magnetic X axes. Orientation of radical C11 in liquid crystals is possibly caused by both its elongated shape and specific guest–matrix interaction. It is known that substance C11 itself is a paramagnetic thermotropic liquid crystal.^{32,33} Thus, it is reasonable to suppose that this radical can be effectively embedded into the liquid crystal matrices.

The lowest order parameters were demonstrated by radical TEMPOL. It is not surprising since the shape of this probe is nearly spherical and it has no aromatic system capable of π – π stacking with the molecules of the liquid crystal.

Molecular Orientation Axes of the Nitroxides Studied.

The values of angles θ and φ , that describe the direction of the preferential orientation axis of the nitroxide molecule in a g -tensor reference frame, are provided in Table 2. θ is an angle between the orientation axis and axis g_{zz} which is directed along the p -orbitals of the nitrogen and oxygen atoms of the paramagnetic fragment. φ is an angle between the projection of the orientation axis on plane g_{xx} – g_{yy} and axis g_{xx} coinciding with the N–O bond (Figure 6a). Thus, the direction of the orientation

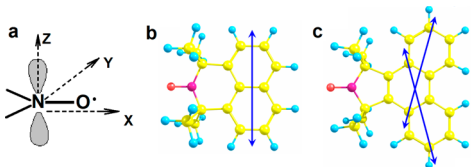


Figure 6. Magnetic axes of nitroxides (a) and molecular orientation axes for radicals A5 (b) and A4(c).

axis was determined relative to the magnetic axes of the nitroxide moiety.

For a reliable determination of the main orientation axis, the geometry of the nitroxide molecule, optimized by means of quantum chemical calculations, was used. It was shown above

that each probe used is sufficiently rigid and characterized mainly by unique molecular geometry. The only probe which has several conformations is the C11 molecule. All conformers of this molecule, nevertheless, have similar molecular shape. Thus, we will compare the directions of main orientation axis determined experimentally with the optimal molecular geometry obtained by DFT calculations.

As discussed above, some orientation directions in nitroxide radicals are indistinguishable by EPR spectroscopy. As a result two or more different directions in the molecular frame can be designated as a possible orientation axis. The choice of real orientation axis in the case of such doubt requires additional experimental data or theoretical arguments.

The direction of the orientation axis for radical A5 is shown in Figure 6b. The values of angle θ in the case 5CB as well as 8CB are close to 90° . This implies that the orientation axis lies in the plane of the molecule. The value $\varphi \sim 90^\circ$ indicates that the orientation axis is orthogonal to the N–O bond. In this case, the direction of the orientation axis was determined unambiguously. The uniaxial orientational behavior of this molecule means that all orientations of the molecule with LC director located in the molecular plane perpendicularly the N–O bond are equiprobable. This feature is possibly induced by the π – π interaction of probe molecule with aromatic rings of media, by the specific complexing of N–O bond, or by both these factors together.

In the case of radical A4, the angle θ is equal to 90° ; therefore, the orientation axis lies in the plane of the molecule as in the previous case. Angle φ is determined to be 75° . The axes with $\varphi = 75^\circ, -75^\circ, 105^\circ,$ and -105° are indistinguishable; hence, two directions of orientation axis are determined from the experiment in this case. On the other hand, these two directions are related to each other by elements of symmetry of the molecule. Thus, the orientation axis can also be unambiguously determined in this case.

The possible directions of the orientation axis in the case of radical C11 are shown in Figure 7(a). These directions were

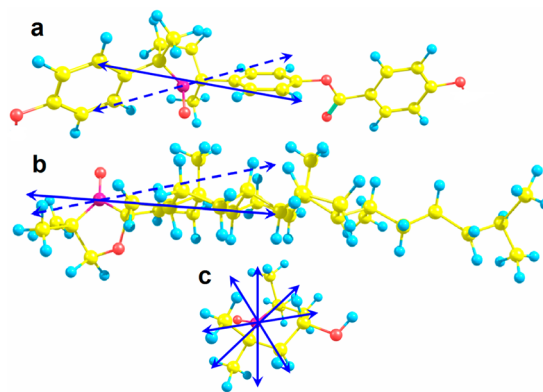


Figure 7. Possible orientation axes for radicals C11 (a), CLS (b), and TEMPOL (c).

determined by the angles θ and φ presented in Table 2. There are two indistinguishable directions of the orientation axis in this case. It is seen however that one of the possible orientation axes is close to the longest geometrical axis of the molecule (solid arrow in the figure). This axis is known to be close to the main rotational axis of the molecule in LC medium.²⁸ Thus, an assignment of the axis directed along the molecule of C11 to the orientation axis seems to be reasonable. The same situation

is seen in Figure 7b for case of radical CLS. Two possible directions of the orientation axis of this radical lie in (CCNO) plane; one of them is directed approximately along the molecule (solid arrow in Figure 7b) and another is tilted to the molecule (dotted line). Probably the true orientation axis is directed along the molecule. The possible orientation axes for radical TEMPOL are shown in Figure 7c. Four different directions correspond to $\theta = \pm 75.5^\circ$ and $\varphi = \pm 65.0^\circ$. Additional data are necessary to make a choice between these directions. Thus, Figure 7 illustrates the cases when additional arguments should be used to convincingly determine the orientational molecular axis.

The directions of the orientation axes in the radicals A3 and A6 are shown in Figure 8a,b. It can be seen that two indistin-

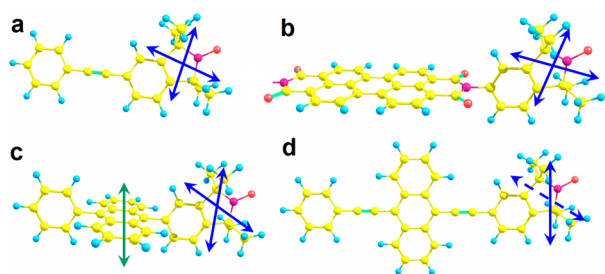


Figure 8. Possible orientation axes for radicals A3 (a), A6 (b), A1 (c), and A2 (d).

guishable directions of the orientation axis corresponding to angles $\pm \varphi$ are in accordance with the local symmetry of the isoindoline fragment of the molecules. Possibly, this feature indicates that the orientation of these molecules is defined by specific properties of the isoindoline moiety, which carries the nitroxide group. Within this assumption, both axes shown in Figure 8a,b are really orientation axes, and these two different orientations of A3 and A6 can be realized in the LC samples simultaneously. However, since molecules A3 and A6 are considerably asymmetrical, it is reasonable to suppose that the statistical weightings of these orientations would be different.

The prospect of the occurrence of two orientations of the probe molecules in LC media is confirmed by the results obtained for radical A1 (Figure 8c). It was shown that radical A1 forms two different orientational distributions. The preferential orientation the set of molecules is characterized by the angles $\theta \sim 90^\circ$ and $\varphi \sim 50^\circ$. Therefore, two possible orientation axes lie in the plane of the isoindoline fragment similar to the orientation axes of radicals A3 and A6. Other molecules are ordered by their Z axes parallel to the LC director (green orientation axis in Figure 8c). The quantum chemical calculations indicate that the planes of isoindoline and phenyl rings form an angle 90° with the plane of the anthracene rings (see Figure 1S in the Supporting Information). In this case, the magnetic Z axis coincides with the direction along the anthracene moiety. As a whole, molecule A1 can be localized in the cyanobiphenyl LC medium by three different modes.

In the case of radical A2 in 5CB, the molecular axes defined by the angles $\theta \sim 90^\circ$ and $\varphi = \pm 58.5^\circ$ are a pair of indistinguishable orientation axes (Figure 8d) directed quite similar to the axes of A1, A3, and A6 radicals. The axis at $\varphi = 58.5^\circ$ additionally coincides with the direction along the anthracene fragment, so this axis is a more probable orientation axis of molecule A2.

A comparison of the results obtained for the same probes in nematic 5CB and smectic 8CB liquid crystals demonstrates that the values of θ and φ for the definite radical are very close in these two matrices. Thus, in this case, the orientational characteristics of the nitroxides are rather insensitive to the type of mesophase.

The data presented here indicate that the orientation axis often does not coincide with the longest molecular axis. Specific interactions of guest and host molecules seem to be a more dominant factor for the orientational ordering of guest molecules. The π - π stacking interaction of condensed aromatic systems of the probes with the benzene rings of liquid crystals molecules should be considered primarily as the possible origin of the specific orientation of guest molecules. Our results show as well that isoindoline fragment is a powerful orienting moiety.

In general it can be concluded that radicals A4, A5, C11, and CLS demonstrate the greatest values of order parameter and uniqueness of orientational axis, and hence, they are the most suitable spin probes for the characterization of the order of liquid crystals.

IV. CONCLUSION

The present work has shown that the direction of the orientation axis of guest paramagnetic molecules in ordered media can be estimated by means of a numerical analysis of the angular dependence of EPR spectra. It was demonstrated that the dominant factor controlling the orientation of a range of guest molecules in ordered media is their specific interactions with the molecules of the matrix. It was found that, depending on the symmetry of magnetic properties of the radical, several possible directions of the orientation axis can be indistinguishable by EPR spectroscopy. The potential for two possible orientations of the probe molecules in LC media was demonstrated. The order parameter values of the nitroxides in the LC matrices were determined up to the 10th rank inclusively. It was shown that the values for order parameters of radicals in nematic 5CB and smectic 8CB are very close. The nitroxide radicals which are the most suitable for characterization of the order of liquid crystals were found to be the more rigid fused systems with limited degrees of intramolecular motions and with prospects for π -stacking with the LC media.

■ ASSOCIATED CONTENT

Supporting Information

Optimized geometries of the radicals under consideration (Cartesian coordinates) as well as energy profiles for intramolecular rotations in radicals A1, A2, A3, A6 and C11. This material is available free of charge via the Internet at <http://pubs.acs.org>

■ AUTHOR INFORMATION

Corresponding Author

*Phone: +74959394900. E-mail: a.kh.vorobiev@gmail.com.

Notes

The authors declare no competing financial interest.

■ ACKNOWLEDGMENTS

The financial support of RFBR (Grant Nos. a-14-03-00323 and mol-a-14-02-31882) and the Australian Research Council Centre of Excellence for Free Radical Chemistry and Biotechnology (CE 0561607) is gratefully acknowledged. Some numerical calculations were performed with the use of the Lomonosov Supercomputer at

Moscow University. We thank Prof. Tatsuhisa Kato (Graduate School of Human and Environmental Studies, Kyoto University) for help in recording the W-band EPR spectra. We thank Dr. Elena Golubeva for helpful discussions.

REFERENCES

- (1) Crawford, G.; Žumer, S. *Cross-Linked Liquid Crystalline Systems: From Rigid Polymer Networks to Elastomers*; Broer, D., Ed.; CRC Press: Boca Raton, 2011.
- (2) Romani, A.; Chidichimo, G.; Formoso, P.; Manfredi, S.; Favaro, G.; Mazzucato, U. Photochromic Behavior of a Spiro-Indolino-Oxazine in Reverse-Mode Polymer-Dispersed Liquid Crystal Films. *J. Phys. Chem. B* **2002**, *106*, 9490–9495.
- (3) Kato, S.; Chen, F.-Q.; Pac, Ch. Anchoring Effect of a Self-Assembled Monolayers for Polymer-Dispersed Liquid Crystal Films. *J. Phys. Chem. B* **2004**, *108*, 320–326.
- (4) Higashiguchi, K.; Yasui, K.; Kikuchi, H. Direct Observation of Polymer-Stabilized Blue Phase I Structure with Confocal Laser Scanning Microscope. *J. Am. Chem. Soc.* **2008**, *130*, 6326–6327.
- (5) Iwata, T.; Suzuki, K.; Amaya, N.; Higuchi, H.; Masunaga, H.; Sasaki, S.; Kikuchi, H. Control of Cross-Linking Polymerization Kinetics and Polymer Aggregated Structure in Polymer-Stabilized Liquid Crystalline Blue Phase. *Macromolecules* **2009**, *42*, 2002–2008.
- (6) Michl, J.; Thulstrup, E. W. *Spectroscopy with Polarized Light: Solute Alignment by Photoselection, in Liquid Crystals, Polymers and Membranes*; VCH Publishers: Deerfield Beach, 1986.
- (7) Chapoy, L. L.; DuPre, D. B. Polarized Fluorescence Measurements of Orientational Order in a Uniaxial Liquid Crystal. *J. Chem. Phys.* **1979**, *70*, 2550–2553.
- (8) Daniels, J. M.; Cladis, P. E.; Finn, P. L.; Powers, L. S.; Smith, J. C.; Filas, R. W.; Goodby, J. W.; Leslie, T. M. Polarization Absorption Spectroscopy: Determination of the Direction and Degree of Orientation of Absorption Transitions. *J. Appl. Phys.* **1982**, *53* (9), 6127–6136.
- (9) Chigrinov, V. G.; Kozenkov, V. M.; Kwok, H.-S. *Photoalignment of Liquid Crystalline Materials: Physics and Applications*; Wiley: Chichester, UK, 2008.
- (10) Bauman, D.; Chrzumnicka, E.; Wolarz, E. Molecular Orientation in Liquid Crystalline Side Chain Polymers Doped with Dichroic Dye as Studied by Optical Spectroscopy Methods. *Mol. Cryst. Liq. Cryst.* **2000**, *352*, 67–76.
- (11) Wolarz, E.; Bauman, D. Study of Orientational Order in a Nematic Polysiloxane by Utilizing the “Guest–Host” Effect. *J. Polym. Sci., Part B: Polym. Phys.* **1993**, *31* (4), 383–387.
- (12) Wolarz, E.; Chrzumnicka, E.; Fischer, T.; Stumpe, J. Orientational Properties of 1,3,4-Oxadiazoles in Liquid-Crystalline Materials Determined by Electronic Absorption and Fluorescence Measurements. *Dyes Pigm.* **2007**, *75*, 753–760.
- (13) Yankova, T. S.; Chumakova, N. A.; Pomogailo, D. A.; Vorobiev, A. Kh. Orientational Order of Guest Molecules in Aligned Liquid Crystal as Measured by EPR and UV–VIS Techniques. *Liq. Cryst.* **2013**, *40* (8), 1135–1145.
- (14) Yankova, T. S.; Bobrovsky, A. Yu.; Vorobiev, A. Kh. Order Parameters P₂, P₄ and P₆ of Aligned Nematic LC-Polymer as Determined by Numerical Simulation of EPR Spectra. *J. Phys. Chem. B* **2012**, *116*, 6010–616.
- (15) Luckhurst, G.; Yeates, R. N. Orientational Order of a Spin Probe Dissolved in Nematic Liquid Crystals An Electron Resonance Investigation. *J. Chem. Soc., Faraday Trans. 2* **1976**, *72*, 996–1009.
- (16) Freed, J. H. Theory of Slow Tumbling ESR Spectra for Nitroxides. In *Spin Labeling: Theory and Applications*; Berliner, L. J., Ed.; Plenum Press: New York, 1976.
- (17) Schneider, D. J.; Freed, J. H. Calculation Slow Motional Magnetic Resonance Spectra: a Users Guide. In *Biological Magnetic Resonance*; Berliner, L. J., Reuben, J., Eds.; Plenum: New York, 1989; Vol. 8.
- (18) Vorobiev, A. Kh.; Chumakova, N. A. Simulation of Rigid-Limit and Slow-Motional EPR Spectra for Extraction of Quantative Dynamic and Orientational Information, In *Nitroxides – Theory, Experiment and Applications*; Kokorin, A. I., Ed.; INTECH: Rijeka, 2012.
- (19) Polnaszek, C. F.; Freed, J. H. Electron Spin Resonance Studies of Anisotropic Ordering, Spin Relaxation, and Slow Tumbling in Liquid Crystalline Solvents. *J. Phys. Chem.* **1975**, *79*, 2283–2306.
- (20) Hwang, J. S.; Rao, K. V. S.; Freed, J. H. An Electron Spin Resonance Study of Pressure Dependence of Ordering and Spin Relaxation in a Liquid Crystalline Solvent. *J. Phys. Chem.* **1976**, *80*, 1490–1501.
- (21) Vorobiev, A. Kh.; Chumakova, N. A. Determination of Orientation Distribution Function of Anisotropic Paramagnetic Species by Analysis of EPR Spectra Angular Dependence. *J. Magn. Reson.* **2005**, *175*, 146–157.
- (22) Vorob'ev, A. Kh.; Chumakova, N. A. Determination of Molecular Orientation Distribution of a Stable Paramagnetic Probe in Oriented 4-Cyano-4'-n-pentylbiphenyl. *Russ. Chem. Bull.* **2005**, *54*, 195–200.
- (23) James, P. G.; Luckhurst, G. R. The Anisotropic Pseudo-Potential of Nematic Liquid Crystals. *Mol. Phys.* **1970**, *19* (4), 489–500.
- (24) Diehl, P.; Schwerdtfeger, C. F. ESR Determination of the Orientation Distribution Function of Vanadyl Acetylacetonate Dissolved in a Liquid Crystal. *Mol. Phys.* **1969**, *17* (4), 423–424.
- (25) Kirov, N.; Fontana, M. P.; Cavatorta, F. Spectroscopic and Thermodynamic Investigation of the Polymorphism of the Solid State of Liquid Crystals. *J. Mol. Struct.* **1980**, *59*, 147–160.
- (26) Kirov, N.; Fontana, M. Determination of Orientational Order Parameter S₂ in Glassy Liquid Crystals by Means of IR Dichroism. *Mol. Cryst. Liq. Cryst.* **1980**, *56* (6), 195–202.
- (27) Kirov, N.; Hadjichristov, G. B.; Fontana, M. P. Vibrational Spectroscopy of Solid Polymorphic Modifications Formed by Thermotropic Liquid Crystals. *J. Mol. Struct.* **2004**, *706*, 65–73.
- (28) Vorobiev, A. Kh.; Yankova, T. S.; Chumakova, N. A. Orientation Distribution Function and Order Parameters of Oriented Spin Probe as Determined by EPR Spectroscopy. *Chem. Phys.* **2012**, *409*, 61–73.
- (29) Horn, R. G. Refractive Indices and Order Parameters of Two Liquid Crystals. *J. Phys.* **1978**, *39*, 105–109.
- (30) Chandrasekhar, S. *Liquid Crystals*; Cambridge University Press: London, 1977.
- (31) Sied, M. B.; Lopez, D. O.; Tamarit, J. Li.; Barrio, M. Liquid Crystal Binary Mixtures 8CB+8OCB: Critical Behavior at the Smectic A – Nematic Transition. *Liq. Cryst.* **2002**, *29*, 57–66.
- (32) Ikuma, N.; Tamura, R.; Shimono, S.; Kawame, N.; Tamada, O.; Sakai, N.; Yamauchi, J.; Yamamoto, Y. Magnetic Properties of All-Organic Liquid Crystals Containing a Chiral Five-Membered Cyclic Nitroxide Unit within the Rigid Core. *Angew. Chem., Int. Ed.* **2004**, *43*, 3677–3682.
- (33) Ikuma, N.; Tamura, R.; Shimono, S.; Uchida, Y.; Masaki, K.; Yamauchi, J.; Aoki, Y.; Nohira, H. Ferroelectric Properties of Paramagnetic, All-Organic, Chiral Nitroxide Radical Liquid Crystals. *Adv. Mater.* **2006**, *18*, 477–480.
- (34) Fairfull-Smith, K. E.; Bottle, S. E. The Synthesis and Physical Properties of Novel Polyaromatic Profluorescent Isoindoline Nitroxide Probes. *Eur. J. Org. Chem.* **2008**, *2008* (32), 5392–5400.
- (35) Keddie, D. J.; Fairfull-Smith, K. E.; Bottle, S. E. The Palladium-Catalysed Copper-Free Sonogashira Coupling of Isoindoline Nitroxides: a Convenient Route to Robust Profluorescent Carbon–Carbon Frameworks. *Org. Biomol. Chem.* **2008**, *6* (17), 3135–3143.
- (36) Micallef, A. S.; Blinco, J. P.; George, G. A.; Reid, D. A.; Rizzardo, E.; Thang, S. H.; Bottle, S. E. The Application of a Novel Profluorescent Nitroxide to Monitor Thermo-Oxidative Degradation of Polypropylene. *Polym. Degrad. Stab.* **2005**, *89*, 427–435.
- (37) Blinco, J. P.; McMurtrie, J. C.; Bottle, S. E. The First Example of an Azaphenylene Profluorescent Nitroxide. *Eur. J. Org. Chem.* **2007**, *2007* (28), 4638–4641.
- (38) Ahn, H.-Y.; Fairfull-Smith, K. E.; Morrow, B. J.; Lussini, V.; Kim, B.; Bondar, M. V.; Bottle, S. E.; Belfield, K. D. Two-Photon Fluorescence Microscopy Imaging of Cellular Oxidative Stress Using Profluorescent Nitroxides. *J. Am. Chem. Soc.* **2012**, *134*, 4721–4730.

(39) Neese, F. *ORCA – an Ab Initio, Density Functional and Semiempirical Program Package, Version 2.4*; Max-Planck-Institut für Bioanorganische Chemie: Mülheim and der Ruhr, 2004.

(40) Barone, V.; Cimino, P.; Stendardo, E. Development and Validation of the B3LYP/N07D Computational Model for Structural Parameter and Magnetic Tensors of Large Free Radicals. *J. Chem. Theory Comput.* **2008**, *4*, 751–764.

(41) *Handbook of Chemistry and Physics*, 33rd ed.; Hodgman, C. D., Ed.; CRC Press: Cleveland, OH, 1951.

(42) Ciunik, Z. Relationship between Electron Difference-Density Distribution, Planarity of the N-O Groups and Intermolecular Hydrogen Bond Systems in Crystals of Stable Nitroxide Radicals. *J. Mol. Struct.* **1997**, *412*, 27–37.

(43) <http://www.chem.msu.ru/eng/lab/chemkin/ODF3/>.

(44) Dennis, J. E.; Gay, D. M.; Welseh, R. E. An Adaptive Nonlinear Least-Squares Algorithm. *ACM Trans. Math. Software* **1981**, *7* (3), 348–383.

(45) Lebedev, Ya. S.; Grinberg, O. Ya.; Dubinsky, A. A.; Poluektov, O. G. Investigation of Spin Labels and Probes by Millimeter Band EPR. In *Bioactive Spin Labels*; Zhdanov, R. I., Ed.; Springer-Verlag: Berlin, 1992.

(46) Barnes, J. P.; Freed, J. H. Dynamics and Ordering in Mixed Model Membranes of Dimyristoylphosphatidylcholine and Dimyristoylphosphatidylserine: A 250-GHz Electron Spin Resonance Study Using Cholestane. *Biophys. J.* **1998**, *75*, 2532–2546.

(47) Zannoni, C. Distribution Functions and Order Parameters. In *The Molecular Physics of Liquid Crystals*; Luckhurst, G. R., Gray, G. W., Eds.; Academic Press: London, 1979.

(48) Shunsuke, T.; Hiroshi, Y. Glass Transition of Liquid-crystalline 4-Alkoxyphenyl and 4-Cyanophenyl 4-(2,4-Dialkoxybenzoyloxy) Benzoates. *J. Chem. Soc., Faraday Trans.* **1994**, *90* (11), 1537–1540.

(49) Buka, A.; de Jeu, W. H. Diamagnetism and Orientation Order of Nematic Liquid Crystals. *J. Phys. (Paris)* **1982**, *43*, 361–367.

(50) Wu, Sh.-T. Infrared Markers for Determining the Order Parameters of Uniaxial Liquid Crystals. *Appl. Opt.* **1987**, *26*, 3434–3440.

(51) Cui, M.; Kelly, J. R. Temperature Dependence of Visco-Elastic Properties of 5CB. *Mol. Cryst. Liq. Cryst.* **1999**, *331*, 49–57.

(52) Magnuson, M. L.; Fung, B. M. On the Temperature Dependence of the Order Parameter of Liquid Crystals over a Wide Nematic Range. *Liq. Cryst.* **1995**, *19*, 823–832.

(53) Luckhurst, G. R.; Yeates, R. N. Orientation Order of a Spin Probe Dissolved in Nematic Liquid Crystal. *J. Chem. Soc., Faraday Trans. 2* **1976**, *72*, 996–1009.

(54) Miyano, K. Raman Depolarization Ratios and Order Parameters of a Nematic Liquid Crystal. *J. Chem. Phys.* **1978**, *69*, 4807–4813.

(55) Ratchkevitch, V. S.; Yakovenko, S. Y.; Pelzl, J. Orientation Characteristics of Liquid Crystals (5cb) by Means of Optical Study. *Liq. Cryst.* **1993**, *15*, 591–604.

(56) Southern, C. D.; Gleeson, H. F. Using the Full Raman Depolarization in the Determination of the Order Parameters in Liquid Crystal Systems. *Eur. Phys. J. E* **2007**, *24*, 119–127.